

## Towards improved floor spectra estimates for seismic design

Timothy J Sullivan<sup>\*1</sup>, Paolo M Calvi<sup>2</sup> and Roberto Nascimbene<sup>2</sup>

<sup>1</sup>*Department of Civil Engineering and Architecture, Università degli Studi di Pavia, Via Ferrata 1, Pavia, 27100, Italy*

<sup>2</sup>*Department of Civil Engineering and Architecture, Università degli Studi di Pavia, Via Ferrata 1, Pavia, 27100, Italy*

*(Received June 2, 2011, Revised March 17, 2012, Accepted May 9, 2012)*

**Abstract.** Current codes incorporate simplified methods for the prediction of acceleration demands on secondary structural and non-structural elements at different levels of a building. While the use of simple analysis methods should be advocated, damage to both secondary structural and non-structural elements in recent earthquakes have highlighted the need for improved design procedures for such elements. In order to take a step towards the formation of accurate but simplified methods of predicting floor spectra, this work examines the floor spectra on elastic and inelastic single-degree of freedom systems subject to accelerograms of varying seismic intensity. After identifying the factors that appear to affect the shape and intensity of acceleration demands on secondary structural and non-structural elements, a new series of calibrated equations are proposed to predict floor spectra on single degree of freedom supporting structures. The approach uses concepts of dynamics and inelasticity to define the shape and intensity of the floor spectra at different levels of damping. The results of non-linear time-history analyses of a series of single-degree of freedom supporting structures indicate that the new methodology is very promising. Future research will aim to extend the methodology to multi-degree of freedom supporting structures and run additional verification studies.

**Keywords:** floor spectra; non-structural elements; secondary structural elements.

---

### 1. Introduction

Recent earthquakes, such as the Darfield earthquake of September 2010 (Dhakai 2010), as well as significant earthquakes from the past, such as the Northridge earthquake of 1994 (Villaverde 1997), have indicated that even if modern seismic design techniques may be able to successfully limit the damage to main structural elements during intense earthquakes, the damage to secondary structural and non-structural elements may be extensive, very costly and in some cases even life threatening. In the 2010 M7.1 Darfield (New Zealand) earthquake, that imposed seismic demands similar to the design code level for the ultimate limit state in the Christchurch region, total losses have been estimated at NZ\$5billion (The Treasury, Government of New Zealand 2011) even though there was no loss of life. Good seismic design of secondary structural and non-structural

---

<sup>\*</sup>Corresponding author, Ph.D., E-mail: [timothy.sullivan@unipv.it](mailto:timothy.sullivan@unipv.it)

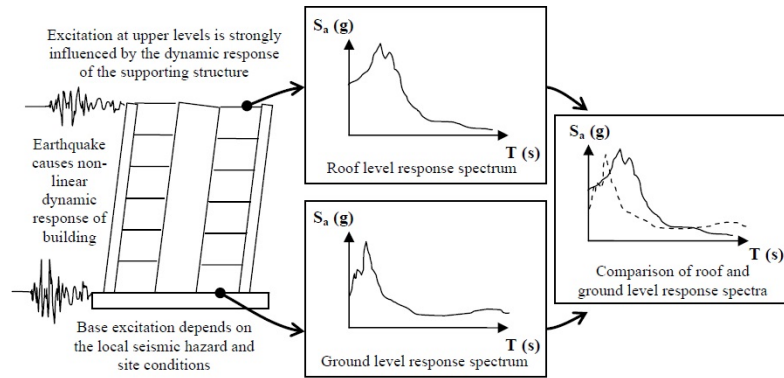


Fig. 1 Illustration of roof and ground level response spectra

elements requires consideration of both the accelerations and deformations imposed on such elements. Deformations can usually be limited through stiffening of the main structural system and then sustained through adequate detailing of the secondary and non-structural elements. If a structure is stiffened, however, it will tend to attract greater acceleration demands (that can be limited somewhat by ductile non-linear response) such that designers are typically faced with a trade off between increased stiffness, to limit displacement demands, and reduced stiffness to limit acceleration demands. In practice, the stiffness and strength of the main structure are usually set to satisfy deformation limits and then floor spectra are established in order to identify the design accelerations for secondary structural and non-structural elements. To this extent, note that the acceleration spectrum at the base of a building will tend to be very different from the acceleration spectra in the upper levels of the structure, as is illustrated in Fig. 1, because the dynamic response of the supporting structure will filter different frequencies of the excitation, amplifying demands in specific period ranges. Note that the floor spectra indicated in Fig. 1 may not be more narrow-banded than the ground level spectra because the inelastic response of the supporting structure causes frequency shifts due to non-linearity, as will be discussed further later in the paper.

International seismic design codes provide different recommendations for the estimation of floor response spectra during design. In the Eurocode 8 (CEN EC8 2004) the acceleration demand,  $S_a$ , acting on a non-structural element of a building can be obtained from

$$S_a = a_g \cdot S \cdot \left( \frac{3(1 + z/H)}{1 + (1 - T_a/T_n)^2} - 0.5 \right) \geq a_g \cdot S \quad (1)$$

where  $a_g$  is the design ground acceleration (in units of g) for a rock site,  $S$  is a modification factor to account for other soil site conditions,  $z$  is the height of the non-structural element above the ground level,  $H$  is the total height of the building,  $T_a$  is the period of the non-structural element and  $T_n$  (denoted  $T_1$  in Eurocode 8) is the natural (first-mode) period of the building in the relevant direction of excitation.

At roof level, Eq. (1) suggests that the peak elastic acceleration imposed on a non-structural element (obtained when  $T_a = T_1$ ) will be 5.5 times the peak ground acceleration (PGA) at the site. Similarly, the New Zealand standard NZS1170.5 predicts a maximum acceleration on non-structural elements (or “parts”) at roof level of 6.0 times the PGA, but unlike Eurocode 8 (EC8),

the peak acceleration does not depend on the period of the supporting structure and instead depends only on the period of the non-structural element (being a maximum for periods of up to 0.75 s). This recommendation appears to stem from the findings of Drake and Bachman (1995), Rodriguez *et al.* (2000) and Shelton *et al.* (2002), who found that acceleration demands are not necessarily dominated by the response of the building's first mode of vibration.

According to the U.S. code ASCE7-05 (2005), the maximum roof level acceleration demand on a non-structural element could be predicted as being 7.5 times the PGA, but the code does impose a limit on the maximum design force that approximately corresponds to a maximum acceleration of 4.0 times the PGA. Note that acceleration demands according to the ASCE7-05 are neither a function of the period of the building nor the period of the non-structural element, but the code acceleration values do distinguish between rigid and flexible components.

The fact that none of these international seismic design codes recommend the same approach for the determination of acceleration demands on non-structural elements suggests that the three code approaches are approximate, at best. Theoretically, one might expect the European approach to be more accurate since it tries to quantify the dynamic amplification of seismic demands that occurs when the period of the non-structural element corresponds to the period of the supporting structure. However, this paper will show that the EC8 approach is not particularly reliable, failing to adequately predict the acceleration demands at the roof level of two different reinforced concrete (RC) wall case study buildings. Note that there are many different approaches proposed in the literature for estimation of floor spectra (Igusa and Der Kiureghian 1985, Villaverde 2004, Taghavi and Miranda 2006, Kumari and Gupta 2007, Menon and Mageses 2008, amongst others). Of those available, the approach of Taghavi and Miranda (2006) is promising, but does require relatively advanced analysis capabilities. The semi-empirical methodology proposed more recently by Menon and Mageses (2008) is simpler and has also been shown to provide good prediction of the out-of-plane demands on Masonry walls, but it does involve the use of numerous equations and calibrated coefficients that render it less appealing to general practicing engineers. Furthermore, most approaches in the literature do not consider the impact of different levels of elastic damping on floor spectra. Given these observations, this work will present a new, simple approach for the prediction of acceleration spectra for the design of secondary structural and non-structural elements on SDOF supporting structures, that sets the peak spectral acceleration demands as a function of the damping of the supported element. Results of NLTH analyses of different period systems will be used to illustrate that the new approach may well be able to improve on current code techniques and should therefore be developed further as part of future research.

## 2. Highlighting the shortcomings of the Eurocode 8 approach

In order to highlight the shortcomings of the EC8 and other code approaches, an 8-storey and a 20-storey cantilever RC wall structure are examined. This section is divided in three parts: firstly, the case study structures are described; secondly, details of the non-linear time-history modelling and analysis approach are provided and finally, the roof level acceleration spectra are reported and compared to the spectra predicted by the code approaches.

### 2.1 Description of the case study RC wall structures

Fig. 2 presents the (part) plan and elevation of the regular 8- and 20-storey case study structures

considered. The lateral load resisting system in each building is provided by a series of relatively long walls in the X-direction and for the purposes of this study, only the response in the X-direction is examined since it is assumed that response in the X-direction will be independent of that in the Y-direction. Material properties are typical of construction practice, with a concrete compressive strength,  $f_{ck}$ , of 25 MPa and reinforcement characteristic yield strength,  $f_{yk}$ , of 450 MPa. The structural layout is considered analogous to a hotel or apartment building in which RC walls act as both partitions and structural elements. This type of structural configuration was selected as it will tend to be stiffer than other types of buildings and should be expected to have higher floor accelerations. Design of the structures was done in accordance with EC8 for the EC8 type 1 spectrum with a ground acceleration of 0.4 g and soil type C. Details of the walls, including reinforcement contents and estimated base flexural strengths, are reported in Table 1. Note that owing to the large number of walls, it was found that design loads were satisfied with the use of minimum quantities of longitudinal reinforcement. The reinforcement detailing for the walls is not shown here but it is assumed that good detailing would be provided in line with the EC8 recommendations to ensure ductile response.

In order to predict the roof level acceleration spectra in accordance with the Eurocode 8 approach of Eq. (1), the fundamental mode period of each structure is required. As such, models of the RC wall structures were developed using Giberson beam elements in Ruaumoko (Carr 2009) in which the cracked section stiffness of the walls was set as 50% of the un-cracked stiffness (which is approximate but agrees with EC8 recommendations) and seismic masses were lumped at floor levels. The first three periods of vibration from eigen-value analyses are reported in Table 2.

## 2.2 Non-linear time-history modeling and analysis approach

In order to investigate the response of the case study structures, a series of non-linear time-

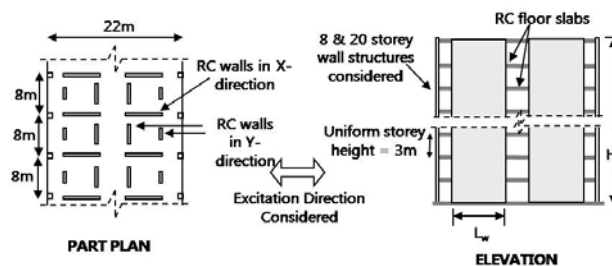


Fig. 2 Illustration of 8-storey and 20-storey case-study RC wall structures

Table 1 Details of the 8-storey and 20-storey RC wall structures

	8-storey	20-storey
Wall length, $L_w$ (m)	8	10
Wall thickness, $t_w$ (m)	0.25	0.25
Seismic Mass per wall (T/floor)	90	90
Wall base axial load (kN)	3200	8800
Longitudinal reinforcement content, $(=A_{sl}/L_w \cdot t_w)$	0.005	0.005
Nominal flexural strength at wall base (kNm)	25540	63070

history (NLTH) analyses were conducted using two-dimensional lumped-plasticity models in Ruaumoko (Carr 2009). Giberson beam elements were used with plastic hinges characterized by the Modified Takeda model (Otani 1981), possessing the base flexural strength values indicated in Table 1 and with post-yield moment-curvature stiffness ratios of 0.025 and 0.030 for the 8-storey and 20-storey structures respectively. The unloading and reloading stiffness was modeled using the Emori and Schonbrich (1978) approach with unloading factors of 0.5 and 0.0 respectively. Plastic hinge lengths were set using the expressions provided by Paulay and Priestley (1992). An integration time-step of 0.001 s was used for the analyses and elastic damping was modeled using a Rayleigh tangent-stiffness proportional damping model with 3% damping imposed on the first mode of vibration and 5% on the 2<sup>nd</sup> mode of vibration. Floors were assumed to behave as rigid diaphragms in-plane, fully flexible out of plane, and consequently nodes at the same level were constrained to move together. The columns and transverse walls (see Fig. 2) were assumed to provide no resistance in the X-direction. The foundations were assumed to behave rigidly and so were not modelled.

A set of 47 accelerograms for the NLTH analyses were selected to match the Eurocode 8 type 1 response spectrum, for a soil type C, corresponding to very stiff soil conditions. A summary of the earthquake characteristics is provided in Table 3, and the acceleration spectra of the records, uniformly scaled to match the EC8 spectrum at a PGA of 0.4g, are presented in Fig. 3. The first seven records listed in Table 3 were taken from the RELUIS data base ([www.reluis.it](http://www.reluis.it)) and the next 40 records were selected from the PEER strong motion database (<http://peer.berkeley.edu/nga/>) except for the Darfield (New Zealand) record which was obtained from the New Zealand GeoNet Strong Motion Data ftp website (<ftp://ftp.geonet.org.nz/strong/processed/Proc>). The set of records is characterized by an average magnitude of 6.6 and distance from the epicenter of 34 km.

Note that while the scale factors reported in Table 3 are for a design PGA of 0.4 g, the accelerograms can also be scaled to match different PGA values for the NLTH analyses, so that the system response under different seismic demand intensities can be investigated. As such, in order to gauge the effects of different seismic intensities on floor response spectra, the NLTH analyses were run for PGA intensity levels of both 0.2 g and 0.4 g, by uniformly scaling the accelerograms by a factor of 0.5 for the 0.2 g PGA scenario.

### 2.3 Roof level response spectra obtained from the NLTH analyses

A roof level response spectrum can be obtained by first establishing the acceleration time-history recorded at the roof level during the NLTH analyses and then using numerical techniques (see Chopra 2000) to establish the corresponding acceleration response spectra. Using Dynaplot (the post-processing program that accompanies the program Ruaumoko, Carr 2009, used here for the NLTH analyses), roof-level response spectra were generated following each NLTH analysis. Note that floor response spectra can be developed for different values of elastic damping that the non-structural elements might be assumed to possess and so both 2% and 5% damped spectra were developed in this phase of the research. While values of the elastic damping of secondary

Table 2 Periods of vibration (X-direction) for the 8- and 20-storey structures

	8-storey	20-storey
First mode period of vibration, $T_1$ (s)	0.557	2.31
Second mode period of vibration, $T_2$ (s)	0.100	0.38
Third mode period of vibration, $T_3$ (s)	0.042	0.14

Table 3 Characteristics of the accelerograms selected for the NLTH analyses

Earthquake name	Date	M <sub>w</sub>	Station	Epicentral distance (km)	Scaling factor	Significant duration (s)
Adana	1998	6.3	ST549	30	4.84	10.74
Izmit	1999	7.6	ST772	20	1.59	12.88
Friuli aftershock	1976	6	ST33	9	12.35	15.4
Alkion	1981	6.6	ST122	19	1.44	10.54
Dinar	1995	6.4	ST271	8	1.88	8.7
Lazio Abruzzo aftershock	1984	5.5	ST152	24	1.7	10.75
Izmit aftershock	1999	5.8	ST3272	26	8.81	15.84
Northridge	1994	6.69	LA - Pico & Sentous	27.8	4.27	15.36
Kobe, Japan	1995	6.9	Shin-Osaka	19.1	2.18	13.32
Friuli, Italy	1976	6.5	Codroipo	33.3	6.18	18.7
Imperial Valley	1979	6.53	Delta	22	1.56	54.95
Chi-Chi, Taiwan	1999	6.2	TCU112	43.5	12.26	30.12
Chi-Chi, Taiwan	1999	6.2	CHY047	38.6	4.13	17.28
Coalinga	1983	6.36	Cantua Creek School	23.8	2.04	12.5
Chi-Chi, Taiwan	1999	6.3	CHY025	39.1	25.19	12.66
Chi-Chi, Taiwan	1999	6.3	CHY036	45.1	2.91	24.42
Chi-Chi, Taiwan	1999	6.3	TCU059	46.7	5.53	29.3
Chi-Chi, Taiwan	1999	6.3	TCU108	41.3	7.99	18.14
Chi-Chi, Taiwan	1999	6.3	TCU123	38.3	5.5	16.75
Morgan Hill	1984	6.19	Hollister Diff Array #3	26.4	6.27	20.9
Morgan Hill	1984	6.19	Hollister Diff Array #4	26.4	5.69	22.2
Morgan Hill	1984	6.19	Hollister Diff Array #5	26.4	6.25	21
Chalfant Valley	1986	6.19	Bishop-LADWP South St	14.4	2.62	11.17
Superstition Hills	1987	6.54	Brawley Airport	17	4.48	13
Superstition Hills	1987	6.54	Kornbloom Road (temp)	18.5	3.77	13.84
Superstition Hills	1987	6.54	Poe Road (temp)	11.2	1.73	13
Spitak, Armenia	1988	6.77	Gukasian	24	3.21	11.05
Loma Prieta	1989	6.93	Fremont-Emerson Court	39.7	3.91	14.12
Loma Prieta	1989	6.93	Gilroy Array #2	10.4	1.66	13.15
Loma Prieta	1989	6.93	Gilroy Array #4	13.8	1.88	17.87
Loma Prieta	1989	6.93	Halls Valley	30.2	4.43	13.65
Loma Prieta	1989	6.93	Hollister Diff. Array	24.5	1.7	10.07
Big Bear	1992	6.46	San Bernardino-E& Hosp.	34.2	4.48	25.87
Northridge-01	1994	6.69	Camarillo	34.8	3.71	12.66
Northridge-01	1994	6.69	Hollywood-Willoughby Ave	17.8	2.56	17.6
Northridge-01	1994	6.69	LA-Baldwin Hills	23.5	2.72	14.52
Northridge-01	1994	6.69	LA-Century City CC North	15.5	2.22	32.44
Denali, Alaska	2002	7.9	R109 (temp)	43	6.5	23.69
Chi-Chi, Taiwan	1999	7.62	TCU085	58	5.8	19.97
Chi-Chi, Taiwan	1999	7.62	TAP065	122	6.1	23.4
Chi-Chi, Taiwan	1999	7.62	KAU003	114	5.2	59.98
Darfield, NZ	2010	7.1	Rata Peats (RPZ)	93	13.4	24.36
Loma Prieta	1989	6.93	So. San Francisco, Sierra Pt.	63	7.2	12.14
Loma Prieta	1989	6.93	So. San Francisco, Sierra Pt.	63	6.8	9.54
Irpinia, Italy-01	1989	6.9	Auletta	10	7.9	18.96
Northridge-01	1994	6.69	Sandberg-Bald Mtn	42	6.2	15.92
Northridge-01	1994	6.69	Antelope Buttes	47	12.7	15.16

structural and non-structural elements should be an area for future research, one could certainly expect values to range from around 1% to 2% for systems such as glass facadè systems (Nakagami

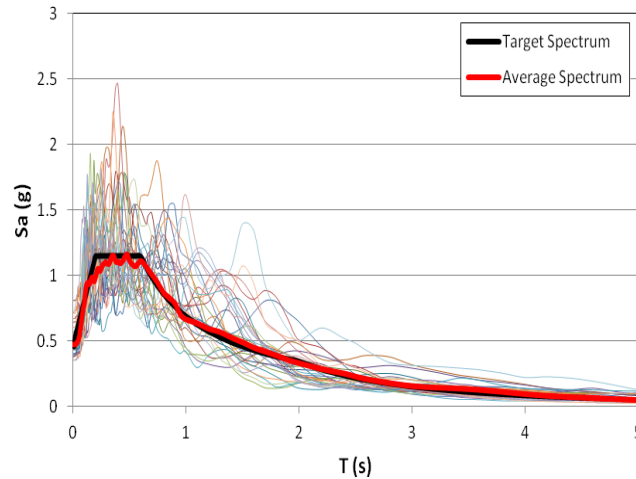


Fig. 3 Acceleration response spectra at 5% elastic damping for the selected accelerograms, scaled to be spectrum compatible with the EC8 type 1 spectrum for soil type C and a PGA = 0.4g

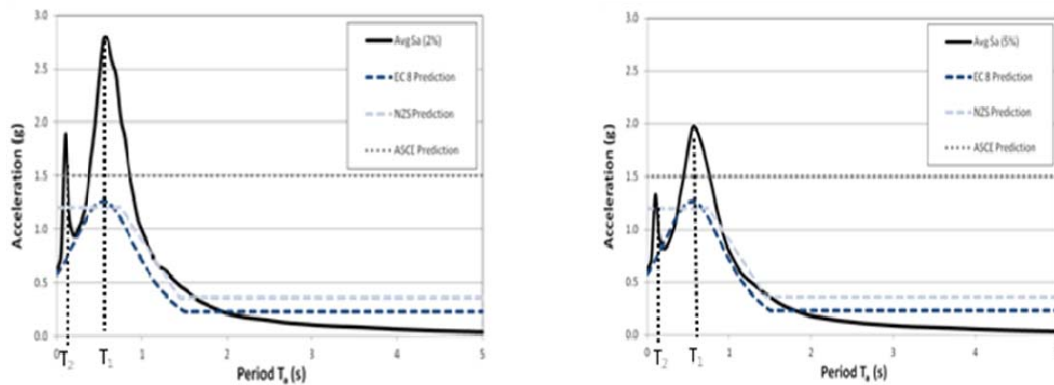


Fig. 4 Comparison of roof level response spectra at 2% (left) and 5% (right) damping predicted via the EC8 approach (Eq. 1) and via NLTH analyses of an 8-storey structure subject to accelerograms compatible with the EC8 spectrum at a PGA=0.2 g

2003, Lenk and Coult 2010, Lago and Sullivan 2011) or steel racks (Krawinkler *et al.* 1979) up to possibly 10% or more for masonry (Magenes *et al.* 2008) or timber partitions (Filiatrault *et al.* 2004) and therefore spectra should be capable of accounting for the likely damping level.

Figs. 4 and 5 present the average of the roof level spectra obtained for the 8-storey and 20-storey structures respectively. Note that the response spectra shown for the 8-storey structure are those obtained using the accelerogram set scaled to an equivalent PGA of 0.2 g, whereas the response spectra for the 20-storey structure correspond to a PGA of 0.4 g. These different intensity levels are selected to best highlight the discrepancies between code predictions and observed accelerations for the case study structures. Note that the EC8 prediction was made according to Eq. (1). According to the ASCE, design forces on non-structural elements will vary according to the type of non-structural element and in this work the most conservative situation has been adopted to establish equivalent acceleration demands for predictions in Figs. 4 and 5.

Conservative criteria were also adopted for the NZS1170 prediction following the requirements

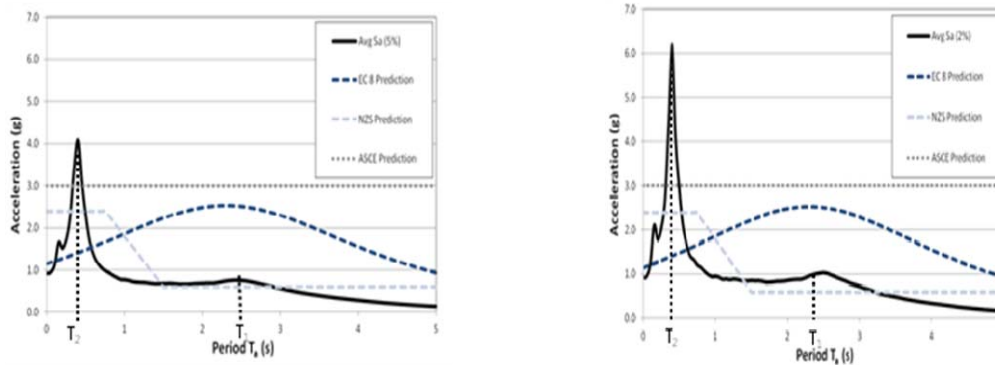


Fig. 5 Comparison of roof level response spectra at 2% (left) and 5% (right) damping predicted via the EC8 approach (Eq.1) and via NLTH analyses of a 20-storey structure subject to accelerograms compatible with the EC8 spectrum at a PGA=0.4 g

for parts and components of the code. The vertical dashed lines indicated on Figs. 4 and 5 show the 1<sup>st</sup> and 2<sup>nd</sup> mode periods of vibration of the case study buildings.

A number of important observations can be made from Figs. 4 and 5. Firstly, note that the roof-level spectral demands predicted by the international codes have underestimated the peak acceleration demands considerably in all cases. Even though the peak acceleration demands observed for the case study structures affect only a narrow period range of the spectrum, they are considered important because there is likely to be uncertainty in the period estimates of both the supporting structure and the supporting element, and the period range over which peak accelerations occur will tend to widen as the inelastic response of the supporting structure increases, as shown later in Section 3.1. The second point to note is that the accelerations at 2% damping are approximately 50% higher than those at 5% damping and this demonstrates that spectral acceleration demands depend on the damping of the non-structural elements. None of the international codes appear to take into account the likely elastic damping of the non-structural elements when estimating the acceleration demands. Thirdly, for the 20-storey structure the shape of the EC8 acceleration spectrum is completely different from that observed. This is considered to be because the EC8 approach only considers amplification of periods associated with the first mode of vibration, whereas the floor spectra can be significantly affected by higher modes of vibration for taller buildings.

Looking at the accelerations predicted by the ASCE, no distinction is made for different period non-structural elements and therefore the ASCE tends to underestimate demands for short period elements and overestimate demands for long period elements. On the other hand, the NZS1170 approach appears to predict the shape of the spectra rather well, but still underestimates the peak acceleration demands in the short period range and does not account for the elastic damping of the supported elements.

Summarising, this section has demonstrated that roof-level acceleration spectra predicted according to code approaches are not accurate for cantilever RC wall structures. Acceleration demands on short-period (up to around 1.0 s) non-structural elements may be greatly underestimated by the code approaches, particularly if the supporting structure has significant higher mode components and the supported element is characterised by low elastic damping. In light of these results, the remainder of this paper will focus on the development of a new means of

estimating floor spectra on single-degree of freedom (SDOF) supporting structures that is capable of accounting for the elastic damping of the supported element. Future research should look to extend the approach to the case of multi-degree of freedom (MDOF) supporting structures and specifically, should identify how to simply construct floor spectra that account for the supporting structure's higher modes of vibration.

### 3. Toward an alternative approach

In order to formulate a new improved means of predicting floor spectra, the floor spectra obtained from NLTH analyses of SDOF supporting structures responding both elastically and inelastically are presented in the next sub-section. A number of analytical considerations are then made to help interpret the results of the NLTH analyses and formulate a new procedure for the prediction of floor spectra.

#### 3.1 Floor spectra for a SDOF supporting structure

A SDOF supporting structure characterized by a fundamental period of 0.6 s has been subject to a series of NLTH analyses using the same modeling approach and accelerograms reported in Section 2.2. In order to examine how the development of inelastic response in the supporting structure would affect the floor spectra, NLTH analyses were conducted for the following three different levels of seismic intensity: (1) PGA = 0.2 g, (2) PGA = 0.4 g and (3) PGA = 0.8 g. Furthermore, spectra were developed for different levels of elastic damping since, as it was shown in the previous section, it can be expected that acceleration demands depend on the assumed damping of the supported system (secondary structural or non-structural element).

Fig. 6 presents the average roof-level floor spectra obtained from the NLTH analyses at the three different intensity levels. The spectra are also plotted for four different values of elastic damping. Note that the response of the supporting structure was close to elastic for the excitation intensity of 0.2 g, developing an average ductility demand of 1.9. The excitation intensities of 0.4 g and 0.8 g developed average peak ductility demands of 4.6 and 9.8 respectively.

As can be seen in Fig. 6, when the supporting structure response is essentially elastic (i.e., for a PGA=0.2 g) the spectra are characterized with a single peak that lies at a period that corresponds

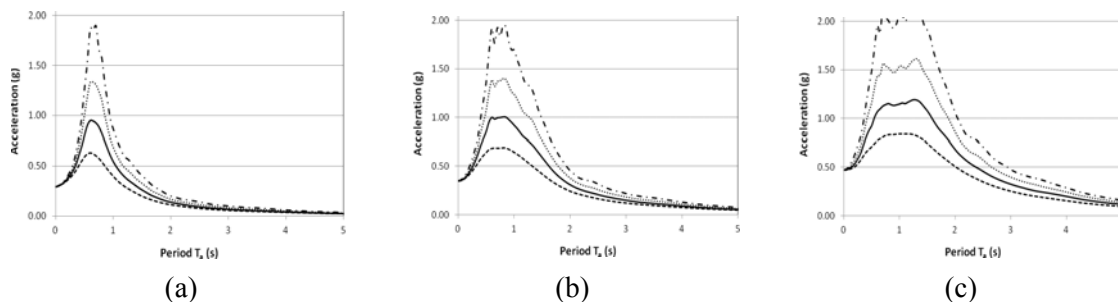


Fig. 6 Roof-level acceleration spectra obtained from NLTH analyses of a SDOF supporting structure using accelerograms compatible with the EC8 type-1 spectrum for (a) a PGA = 0.2 g (b) a PGA = 0.4 g and (c) a PGA = 0.8 g

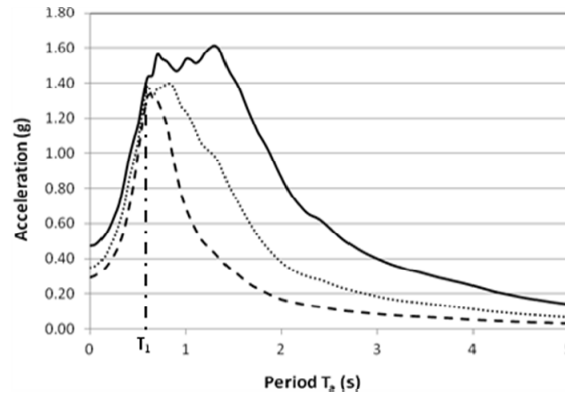


Fig. 7 Comparison of 5% damped roof-level acceleration spectra obtained for a SDOF supporting structure subject to NLTH analyses of increasing intensity

to the elastic fundamental period of the supporting structure. After the peak, the acceleration demands drop off relatively quickly. For higher intensity shaking, for which the supporting structure responds inelastically, it can be seen that the peak of the spectra is no longer so pronounced and instead appears to be a diffused phenomena, involving more than a single period of vibration. The tendency for a spectral acceleration “plateau” to form during the development of non-linear response is even more evident in Fig. 7 where the average spectra at 5% elastic damping are compared for the three different excitation intensities (the dashed vertical line indicates the 1<sup>st</sup> mode period of the supporting system). It is apparent that the peak spectral acceleration demands do not depend on the PGA as international seismic design codes currently suggest. Instead, the peak spectral acceleration appears to be relatively constant, but lies on a wider range of periods as the ductility demand on the supporting structure increases. The reasons for these trends will be explained in the next section.

### 3.2 Interpreting the results: what influences the floor spectra?

In order to formulate an improved methodology for the prediction of floor response spectra, one must understand the physical phenomena influencing the floor spectra. Before proceeding with this discussion, however, it is worth pointing out that this paper will assume that the response of the supporting structure is independent of the response of the supported structure (or non-structural element). This implies that the mass of the supported element is likely to be very low in comparison to the mass of the supporting structure. In addition, this work assumes rigid diaphragm in-plane behavior.

One of the first concepts that should be discussed relates to dynamic amplification of structures subject to harmonic loading. The earthquake excitation of a building will excite its various modes of vibration. Consequently, one could expect the accelerations at roof level to vary harmonically at a frequency corresponding to the natural frequency of the supporting structure. As is demonstrated in many texts on the dynamics of structures (e.g. Thomsen and Dahleh 1998, Chopra 2001), the maximum displacement,  $u_{\max}$ , and acceleration,  $\ddot{u}_{\max}$ , of a structure subject to a harmonic excitation can be obtained from

$$u_{\max} = \frac{F}{k} \cdot \frac{1}{\sqrt{(1-\beta^2)^2 + (2\beta\xi)^2}} = u_0 \cdot DAF_d \quad (2)$$

$$\ddot{u}_{\max} = \frac{F}{m} \cdot \frac{\beta}{\sqrt{(1-\beta^2)^2 + (2\beta\xi)^2}} = \ddot{u}_0 \cdot DAF_a \quad (3)$$

where  $F$  is the peak magnitude of the harmonically applied forcing function,  $k$  is the stiffness of the structural system,  $\beta$  is the ratio of the forcing function period to the structure's period of vibration,  $\xi$  is the elastic damping of the structure and  $m$  is the mass of the structure.  $DAF_d$  and  $DAF_a$  are equivalent dynamic amplification factors for displacement and acceleration respectively.

From Eq. (3) it is apparent that when the period of the forcing function is close to the period of the structure (i.e., as  $\beta$  approaches a value of 1.0), significant dynamic amplification should be expected.

The maximum values of the dynamic amplification coefficients,  $DAF_d$  and  $DAF_a$ , are obtained from Eqs. (2) and (3) for resonant excitation when  $\beta=1.0$ , which gives

$$DAF_d = DAF_a = \frac{1}{2\xi} \quad (4)$$

and it is apparent therefore, that for resonant harmonic excitation, the maximum response is limited only by the damping of the structure.

While these are useful observations for the dynamics of structures subject to harmonic excitation, one would clearly expect the expression to be too conservative for structures subject to seismic shaking since earthquakes do not impose harmonic excitation of infinite duration. However, the authors will later show that the dynamic amplification concept is worth introducing as a potential means of capturing important factors affecting floor response spectra; namely the elastic damping of the supported element and the ratio of the period of the supported element to the period of the supporting structure.

To illustrate how conservative Eq. (4) is for the SDOF supporting structures reported in the previous section, Table 4 compares the apparent dynamic amplification observed from the spectra of Fig. 5 with the dynamic amplification factor (DAF) predicted by Eq. (4). Note that in order to calculate the apparent dynamic amplification factors from the NLTH analysis results, the peak spectral acceleration (of Fig. 5) has been divided by the peak acceleration of the supporting structure's mass.

Table 4 Apparent dynamic amplification factors observed from NLTH analyses compared with those predicted by Eqs. (4) and (5)

Elastic damping	Elastic system	PGA 0.2 g	PGA 0.4 g	PGA 0.8 g	Eq. (4)	Eq. (5)
2%	8.03	6.24	5.57	4.73	25	7.07
5%	5.13	4.40	4.00	3.41	10	4.47
10%	3.36	3.16	2.87	2.53	5	3.16
20%	2.07	2.11	1.97	1.80	2.5	2.24

Comparing the values listed in Table 4, it is evident that the apparent dynamic amplification factors recorded through NLTH analyses are indeed significantly overestimated by Eq. (4), especially for systems characterized by damping ratios of 2% and 5%. As stated earlier, this is because Eq. (4) assumes that a function forcing the system is characterized by an “infinite” duration, with constant amplitude and constant forcing frequency. Of course, for seismic conditions this is not the case and this therefore explains why there are large discrepancies between the theoretical and observed values reported in Table 4.

The apparent dynamic amplification coefficient for use in the construction of floor response spectra could be considered a function of the following three parameters:

- (1) the ratio of the period of vibration of the supporting structure to the period of vibration of the supported element (equivalent to the term in Eqs. (2) and (3));
- (2) the duration of the seismic excitation (or better, the number of forcing cycles);
- (3) the “regularity”, in terms of amplitude, of the seismic excitation itself.

Both the duration (or number of forcing cycles) and the average amplitude of the equivalent forcing function are difficult to define for seismic conditions since they are likely to be sensitive to the ground motion characteristics and characteristics of the supporting structure. Such difficulties help explain why none of the international seismic codes propose the same approach for estimating floor spectra and instead incorporate empirical procedures (even though one should note that the ratio of the period of the non-structural element to the period of the building in Eq. (1) could be considered equivalent to the use of the term in dynamic amplification expressions such as those given by Eqs. (2) and (3)). In this work, the empirical Eq. (5) has been developed and, as can be seen from Fig. 8, it provides a good estimate of the apparent dynamic amplification factor (DAF) values presented earlier in Table 4.

$$DAF = \frac{1}{\sqrt{\xi}} \quad (5)$$

where  $\xi$  is the damping of the supported structure or non-structural element. Note that while improved expressions might be found as part of future research through consideration of a greater number of ground motions and supporting structure characteristics, the results that will be presented in this work indicate that the simple expression given by Eq. (5) may be sufficient for design purposes and will tend to provide better predictions of peak acceleration demands than

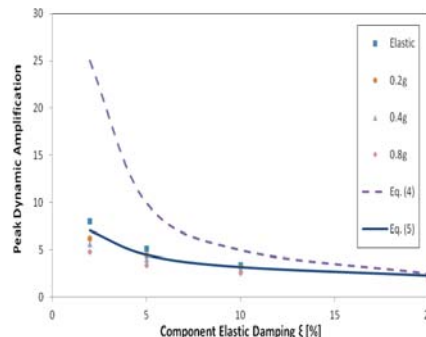


Fig. 8 Comparison of apparent dynamic amplification factors observed through NLTH analyses compared with the values predicted through Eqs. (4) and (5)

current code methods.

The DAF given by Eq. (5) can be used to amplify the maximum floor acceleration of the supporting structure in order to estimate the maximum acceleration imposed on the supported element. For a SDOF supporting system, an upper bound limit to the acceleration of the floor is given by Eq. (6)

$$a_{\max} = \frac{V_b}{M} = \frac{V_y [1 + r(\mu - 1)]}{M} \quad (6)$$

where  $V_b$  is the base shear resistance,  $M$  is the mass of the supporting structure,  $V_y$  is the base shear at yield,  $r$  is the post-yield strain hardening factor (typically 0.05 for RC structures) and is the displacement ductility demand. Eq. (6) is obtained by rearranging Newton's second law (Newton 1687) such that acceleration equals force divided by mass, with the maximum force being equal to the resistance for equilibrium. The increase in lateral force due to strain hardening (the term within square brackets of the numerator) is also obtained from first principles (see Paulay and Priestley 1992). Note that this value is considered valid for SDOF supporting structures but could significantly underestimate the maximum floor accelerations in MDOF supporting structures due to higher mode effects (see Rodriguez *et al.* 2002, Sullivan *et al.* 2006, Rivera 2008). In Sullivan *et al.* (2006) it was observed that the second mode of vibration in frame-wall structures could cause floor acceleration components as large as those from the first mode. As such, Eq. (6) should not be used to predict floor accelerations in MDOF systems, at least not without taking additional steps to account for the higher mode characteristics of the MDOF systems.

By multiplying the acceleration from Eq. (6) by the DAF obtained from Eq. (5), the peak spectral acceleration is obtained. This amplified acceleration value would be expected to occur when the period of the supported element corresponds to the period of vibration of the supporting structure. For SDOF supporting structures it is clear that the relevant period of vibration would be the fundamental frequency of the supporting structure. However, the period of vibration of the supporting structure would be expected to lengthen as inelastic response develops. In addition, for

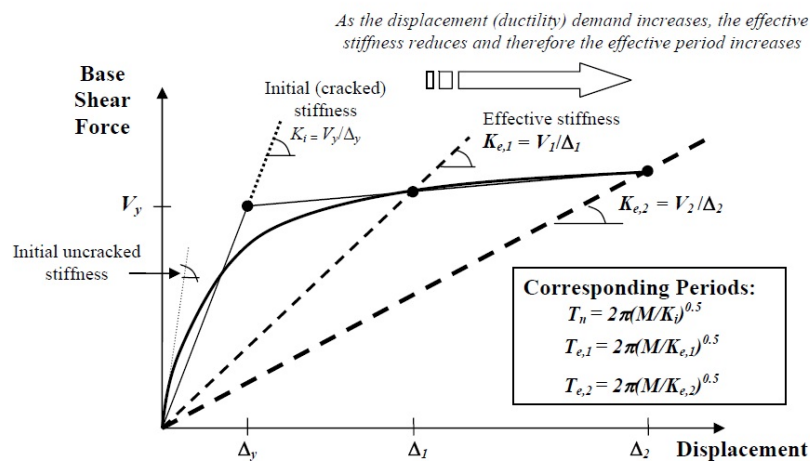


Fig. 9 Force-displacement response of a RC structure, annotated to illustrate concept of the effective stiffness and effective period at two different displacements;  $\Delta_1$  and  $\Delta_2$

MDOF systems, periods associated with higher modes of vibration could also excite the supported structure, suggesting that more than one value of period should be considered. Future research will look to investigate simplified means of dealing with a supporting structure's higher mode contributions to floor spectra.

As was pointed out in the previous section, when the supporting structure responds inelastically there is a tendency for an acceleration plateau to develop in the floor spectra. It was seen in Fig. 7 that the larger the ductility demand on the supporting structure, the wider the plateau. Note that when a SDOF supporting structure yields and non-linear response develops, the maximum acceleration of the floor remains constant, being limited by the maximum force that can develop in the structure, as was explained with reference to Eq. (6). In contrast, significant reductions in the stiffness of the supporting structure occur, and the apparent period of vibration of the structure lengthens. Consequently, because the period of the supporting structure lengthens during the seismic response it is clear that the apparent forcing period on the supported elements should also be expected to lengthen by the same amount. As such, the maximum acceleration given by Eq. (6) could be expected to occur over the period range from the initial fundamental period of the structure through to the effective period of the structure (associated with the secant stiffness at peak response) and this accounts for the apparent plateaus seen earlier in Figs. 6 and 7. Menon and Magenes (2008) provide a similar explanation for the spectral acceleration plateau. Also note that the different stiffness definitions required to define the start and end of the spectral acceleration plateau are illustrated in Fig. 9.

### 3.3 New methodology for the prediction of floor spectra on SDOF supporting structures

The previous sections have identified the factors that affect the peak accelerations of floor spectra. In order to develop an entire spectrum of accelerations, acceleration estimates are also clearly required for the cases where the supported elements do not possess the same period as the supporting structure. If the supported element is very stiff and has low mass, its period will approach zero and therefore the acceleration demands on the element should approach those of the floor itself. In other words, the floor spectral acceleration coordinate at a period of zero ( $T=0$  s) is given by Eq. (6).

Thus, in order to estimate a floor response spectrum it will be assumed that the acceleration for  $T_a=0$  s can be set from Eq. (6) and that the acceleration at  $T_a = T_n$  (where  $T_n$  is the initial natural period of the supporting structure) can be approximated by multiplying the acceleration from Eq. (6) by the dynamic amplification factor from Eq. (5). As the supporting structure period of vibration will tend to lengthen as inelastic response develops (as per Fig. 9) it will be further assumed that acceleration demands remain constant up until  $T_a = T_e$  where  $T_e$  is the effective period (see Fig. 9) that can be approximated by Eq. (7)

$$T_e = T_n \sqrt{\mu} \quad (7)$$

where  $\mu$  is the displacement ductility demand on the SDOF supporting structure. Eq. (7) is based on the observations that, if strain-hardening is negligible, the effective stiffness is equal to the initial stiffness multiplied by the ductility and that the period of vibration of a system is proportional to the inverse square-root of the stiffness (see Priestley *et al.* 2007 for further details). Note that there are different expressions in the literature for the effective period (such as those proposed by Priestley *et al.* 2007 and Menon and Magenes 2008) but Eq. (7) is considered the simplest

expression and will tend to only slightly overestimate the effective period (by 5% for a RC structure subject to a ductility demand of 3.0).

Beyond the effective period of the supporting structure, the acceleration demands should be expected to drop off relatively quickly. The amplified acceleration should again depend on the period ratio and the damping of the supported element. A theoretical upper bound limit to the amplified acceleration at any period could be assumed to be provided by Eq. (3). However, as discussed earlier, the earthquake motion does not apply an infinite number of cycles to the structure and hence for the case the  $\beta = 1$ , the DAF should tend towards Eq. (5). An alternative theoretical approach considered here is the expression (adapted from Thomsen and Dahleh 1998) for a shock spectrum for systems with zero damping subject to a half sine pulse

$$DAF = \frac{1}{1 - \frac{1}{\beta}} \quad (8)$$

where  $\beta$  is the ratio of the forcing function period to the supported element period. This expression for the DAF is of interest since it could indicate the potential effect of a single cycle of seismic response on floor spectra. However, it cannot be used directly to predict dynamic amplification under seismic loading since no adjustment is made for damping, which was shown earlier to be important. Given that a general expression for dynamic amplification under seismic loading could not be found in the literature, Eq. (9) is proposed for the estimation of the dynamic amplification factor for seismic loading conditions

$$DAF = \frac{1}{\sqrt{\left(1 - \frac{1}{\beta}\right)^2 + \xi}} \quad (9)$$

where the symbols are as defined earlier. While Eq. (9) does include terms similar to those in both Eqs. (8) and (5), it has not been theoretically derived and is purely empirical. While the results presented later in this paper suggest that it may be adequate for design purposes, future research should aim to develop a theoretical expression.

At this stage the proposed expressions for the construction of floor spectra on SDOF supporting structures can be introduced as follows

$$\begin{aligned} a_m &= \frac{T_a}{T_y} \cdot [a_{\max} (DAF_{\max} - 1)] + a_{\max} & \text{for } T_a < T_n \\ a_m &= a_{\max} DAF_{\max} & \text{for } T_n \leq T_a \leq T_e \\ a_m &= a_{\max} DAF & \text{for } T_a > T_e \end{aligned} \quad (10)$$

where  $a_m$  is the acceleration spectral coordinate for a supported element of period  $T_a$ ,  $a_{\max}$  is the maximum acceleration of the mass of the supporting structure (given by Eq. (6)),  $T_n$  is the natural (initial) period of the supporting structure,  $T_e$  is the effective period of the supporting structure (given by Eq. (7)),  $DAF$  is the dynamic amplification factor from Eq. (9) with  $\beta = T_e/T_a$ , and  $DAF_{\max}$  is the maximum expected dynamic amplification obtained by substituting  $\beta = 1.0$  into Eq.

(9) or directly from Eq. (5) as  $DAF_{max} = 1/\zeta^{0.5}$ .

Note that the floor spectra expressions propose that in the short period range the accelerations vary linearly. This is proposed in order to provide a simple but acceptably conservative estimate of the acceleration demands in this period range. Also note that the expected ductility demand on the supporting structure is required in order to estimate the effective period. If a Direct displacement-based procedure has been adopted as recommended by Priestley *et al.* (2007), then the ductility demand will be known.

If force-based design is used to design the supporting structure then the ductility demand on the system is not easily established and in this case, designers can use the behaviour (force-reduction) factor as the ductility demand. For example, in line with the EC8 for a single storey RC frame structure 3.5 m high, the designer could estimate a period of vibration equal to  $T_n = 0.2$  s and a behaviour (reduction) factor equal to 4.5. After following a standard force-based design procedure it might be assumed that the designer provides the structure with a design base shear resistance,  $V_y$ , equal to 25% of the building seismic weight; i.e.,  $V_y = 0.25M.g$ , where  $M$  is the seismic mass and  $g$  is a acceleration due to gravity. Inserting this information into Eq. (6), together with a value of  $r = 0.05$ , and assuming the displacement ductility demand equal to the behaviour factor such that  $\mu = 4.5$ , one can estimate the maximum acceleration at roof level,  $a_{max} = 0.25 [1+0.05(4.5-1)].g = 0.425g$ . Using Eq. (7) the designer would then estimate an effective period of  $T_e = T_n \cdot \sqrt{\mu} = 0.42$  s. At this point the designer possesses all the information required to use Eqs. (9) and (10) and therefore can construct roof level spectra for different levels of elastic damping. As such, adapting the procedure to a force-based design situation is relatively straightforward. Nevertheless, implementation within a displacement-based design procedure will lead to better results since both

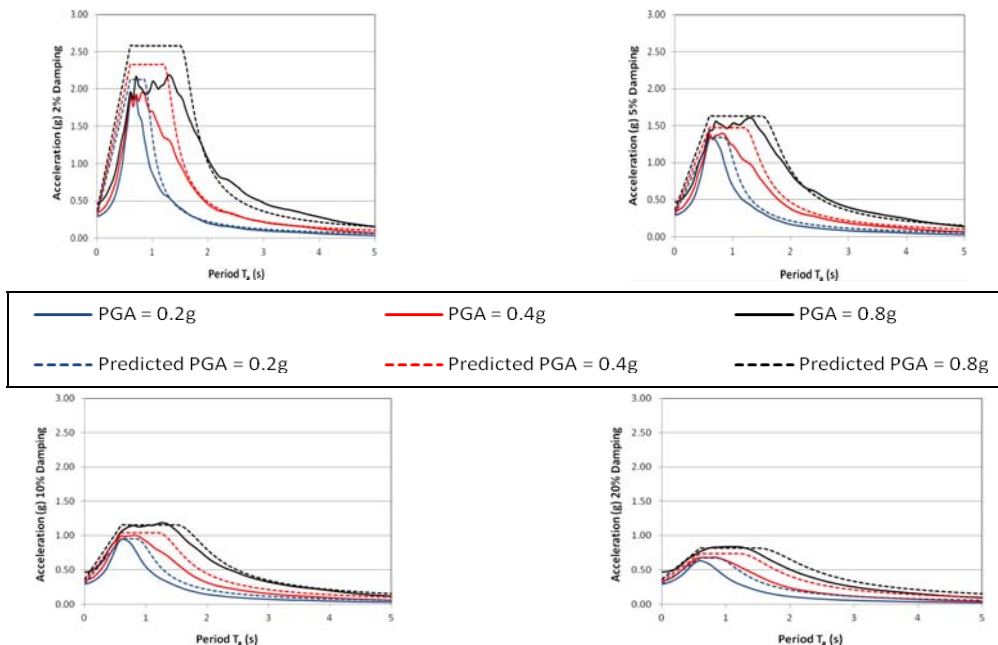


Fig. 10 Comparison of floor spectra at 2%, 5%, 10% and 20% damping predicted by Eq. (10) with those obtained from NLTH analyses of a 0.557 s period SDOF supporting structure using accelerogram set 1 (see Table 3)

the supporting system period and ductility are typically inaccurately estimated using force-based design procedures (see Priestley *et al.* 2007 for clarification).

### 3.4 Verification of the new approach

In order to verify the performance of the new approach for SDOF supporting structures, the floor spectra obtained from the NLTH analyses reported in Section 3.1 are compared with the floor spectra predicted by Eq. (10), as shown in Fig. 10. In addition, as one might expect the amplification to depend on the period of the supporting structure, two other SDOF supporting structures are examined; one with a period of 1.3 s and the other with a period of 2.0 s. The structures are again modelled in Ruaumoko (Carr 2009) using a lumped plasticity approach with Takeda hysteretic characteristics and with plastic hinge strengths set to provide approximately elastic response for a  $PGA = 0.2$  g. NLTH analyses are conducted using the same set of accelerograms listed earlier in Table 3. Figs. 11 and 12 compare the floor spectra obtained from NLTH analyses with those predicted by Eq. (10) for the 1.3 s and 2.0 s SDOF supporting structures respectively.

The results illustrated in Figs. 10 to 12 illustrate that the new approach provides an effective means on predicting floor spectra since the spectral plateaus and the general shape of the spectra

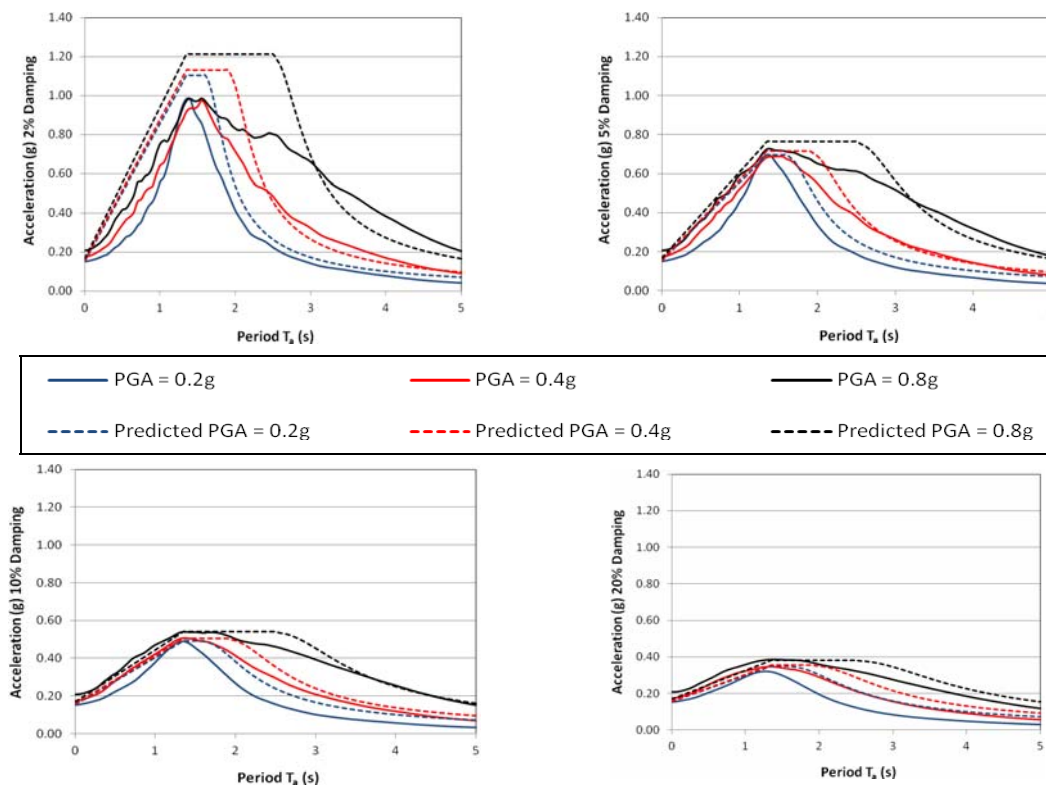


Fig. 11 Comparison of floor spectra at 2%, 5%, 10% and 20% damping predicted by Eq. (10) with those obtained from NLTH analyses of a 1.33 s period SDOF supporting structure using accelerogram set 1 (refer Table 3)

are well predicted, even for different levels of damping and seismic intensity. One can note that as the inelastic demands on the supporting structure increase (i.e., as the PGA increases here), the predicted spectra do tend to be slightly conservative and future research might explore the possibility of finishing the spectral plateau at periods slightly smaller than the effective period. This could be particularly important for the correct prediction of spectral displacement demands on secondary or non-structural elements.

#### 4. Investigating the influence of ground motion characteristics on peak floor acceleration demands

The research findings presented to this point have illustrated that the peak floor spectral acceleration demands should depend on the elastic damping of the non-structural component and the apparent dynamic amplification can be well approximated using Eq. (5). However, as mentioned earlier in Section 3.2, the empirical amplification expression Eq. (5) could be sensitive to ground motion characteristics. In order to gauge the sensitivity of the peak spectral acceleration demands to the ground motion characteristics, this section presents apparent amplification factors

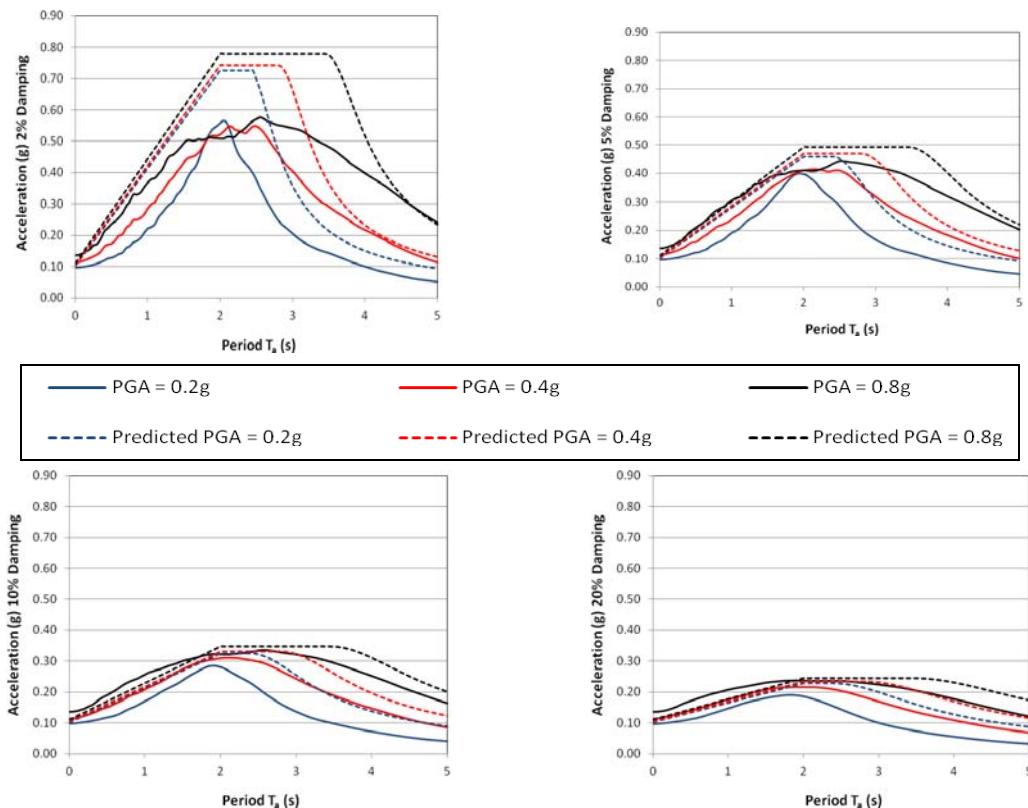


Fig. 12 Comparison of floor spectra at 2%, 5%, 10% and 20% damping predicted by Eq. (10) with those obtained from NLTH analyses of a 2.0 s period SDOF supporting structure using accelerogram set 1 (refer Table 3)

obtained using a set of ground motions characterised by long duration and a set of near-field ground motions characterised by velocity pulses.

#### 4.1 Long duration ground motions

The duration of ground motion shaking could be expected to significantly affect the apparent dynamic amplification since such long duration ground motions will subject the structure to a greater number of cycles, increasing the probability that a resonant type of response will develop, thereby leading to greater dynamic amplification. In this work, the apparent dynamic amplification factors obtained from the twelve long duration ground motions listed in Table 5 are examined. Note that the significant duration of the ground motions reported in Table 5 corresponds to the interval of time between which 5% and 95% of the total Arias Intensity is accumulated (see Kramer, 1996 for details) and was determined using the software Seismosignal (Seismosoft 2011).

Since the impact of duration might be expected to be more relevant for certain periods of vibration, seven damped elastic SDOF systems characterized by periods of vibration equal to 0.3, 0.6, 1.2, 1.8, 2.4, 3 and 3.6 seconds are selected as supporting structures in this section. The structures are modelled using the same approach described in Section 2.2 but only elastic supporting-structure response is considered. Floor spectra are obtained for four component damping values of 2%, 5%, 10% and 20% of the critical damping. Fig. 13(a) presents the apparent dynamic amplification factors at 5% damping obtained for the different period systems and compares the factors with those predicted by Eqs. (4) and (5) as well as international code approaches. The amplification factors for international codes were obtained by dividing the peak spectral acceleration prescribed by the code for non-structural elements possessing a period of vibration equal to that of the supporting structure by the peak acceleration of the supporting structure. Fig. 13(b) compares the 50<sup>th</sup> percentile values for the observed dynamic amplification factors with those predicted by Eqs. (4) and (5).

Table 5 Details of the accelerograms selected to study the effect of duration on floor response spectra

Earthquake name	Date	$M_w$	Station name	PGA (g)	Duration (s)	Significant duration (s)
Chile, NS	2010	8.8	Colegio San Pedro	0.65	101	36
Chile, NS	2010	8.8	Colegio San Pedro	0.61	101	36
Sumatra, NS	2007	8.4	Sikuai Island, West Sumatra	0.04	129	47
Sumatra, EW	2007	8.4	Sikuai Island, West Sumatra	0.04	129	47
Chile, NS	1985	8	Llolleo	0.71	116	37
Chile, EW	1985	6.9	Llolleo	0.71	116	37
Mexico, EW	1985	8.3	SCT	0.17	180	38
Mexico, NS	1985	8.3	SCT	0.11	180	38
Japan, EW	2011	9	IWT008	0.33	300	79
Japan, NS	2011	9	IWT008	0.25	300	79
Japan, EW	2011	9	MYG011	0.68	300	105
Japan, NS	2011	9	MYG011	0.92	300	105

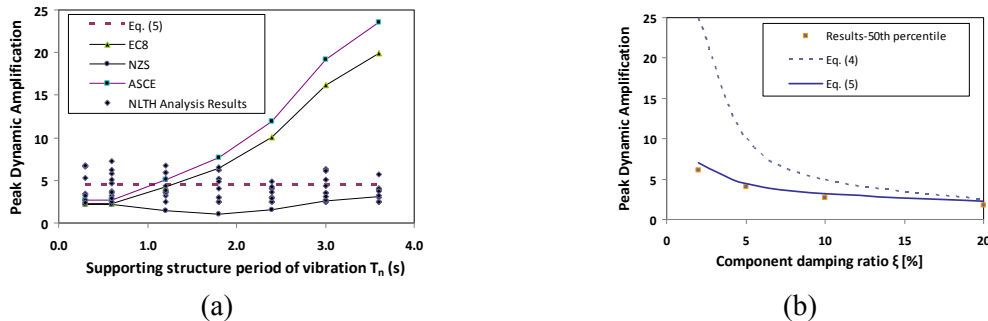


Fig. 13 Apparent dynamic amplification factors obtained using long duration ground motions for (a) 5% elastic damping and supporting structures of varying period and (b) 2%, 5%, 10% and 20% damping together with predictions from Eqs. (4) and (5)

Table 6 Details of ground motions from near-source events with pulse periods between 1.0 s and 2.0 s (from Baker 2007)

Earthquake name	Date	$M_w$	Station	Pulse period $T_p$ (s)
Mammoth Lakes-10	1983	5.34	Convict Creek	1.55
Morgan Hill	1984	6.19	Hollister Diff Array #1	1.28
Morgan Hill	1984	6.19	Hollister Diff Array #6	1.24
Kobe	1995	6.90	Takatori	1.62
Kobe	1995	6.90	Takarazuka	1.43
Coyote Lake	1979	5.74	Gilroy Array #6	1.21
Sierra Madre	1991	5.61	San Marino - SW Academy	1.04
Sierra Madre	1991	5.61	LA - City Terrace	1.18
San Fernando	1971	6.61	Pacoima Dam (upper left abut)	1.6
San Fernando	1971	6.61	Lake Hughes #1	1.15
San Fernando	1971	6.61	Lake Hughes #4	1.05
N. Palm Springs	1986	6.06	N PALM SPR P.O.	1.38
Northridge-01	1994	6.69	Rinaldi Receiving Sta	1.23
Irpinia Eq.	1980	6.90	Bagnoli Irpinio	1.76
Northridge	1994	6.7	Century City LACC North	1.62
Northridge	1994	6.7	LA Dam	1.65

The results presented in Fig. 13 suggest that long duration ground motions are relatively well predicted by the empirical Eq. (5). The trends observed in Fig. 13 are somewhat surprising because they suggest that long duration ground motions do not develop larger dynamic amplification factors than normal duration ground motions, despite the fact that they impose a greater number of cycles of excitation on the structure. The authors believe that this occurs because not only the number of cycles affects dynamic amplification but also the regularity in the amplitude of the excitation. For instance, one could find that five cycles of excitation at the same magnitude leads to significantly greater dynamic amplification than ten cycles of varying amplitude. The variability in amplitude that characterises normal duration accelerograms may well be similar to that characterising long duration accelerograms, and consequently the dynamic amplification factors obtained with the two sets of ground motions are similar. This point should be investigated further

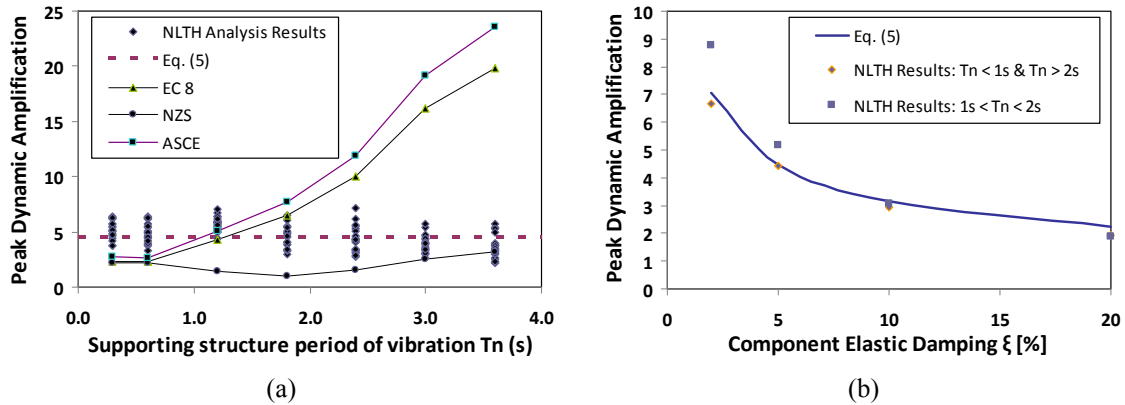


Fig. 14 Apparent dynamic amplification factors obtained using near-source ground motions for (a) 5% elastic damping and supporting structures of varying period and (b) 2%, 5%, 10% and 20% damping together with predictions from Eq. (5)

as part of future research. However, the results presented in this section do suggest that Eq. (5) may even be suitable for use with long duration earthquakes.

#### 4.2 Near-source ground motions

Just as long duration ground motions might be expected to significantly affect the apparent dynamic amplification factors, so too might short duration records with significant pulse-type characteristics. In this work, the 16 accelerograms listed in Table 5 are used to examine the apparent dynamic amplification factors obtained for records with velocity pulses. The dataset is a subset of fault-normal and fault parallel rotated records from the next generation attenuation project (NGA) database analysed by Baker (2007). Note that the records examined possess pulse periods between 1.0 and 2.0 s, identified by Baker (2007).

As the impact of pulse period should be expected to be more relevant for certain periods of vibration, seven damped elastic SDOF systems characterized by periods of vibration equal to 0.3, 0.6, 1.2, 1.8, 2.4, 3 and 3.6 seconds are again selected as supporting structures in this section. The structures are modelled using the same approach described in Section 2.2 but only elastic supporting-structure response is considered. Floor spectra are obtained for four component damping values of 2%, 5%, 10% and 20% of the critical damping. Fig. 14(a) presents the apparent dynamic amplification factors at 5% damping obtained for the different period systems and compares the factors with those predicted by Eqs. (4) and (5) as well as international code approaches. The amplification factors for international codes were again obtained by dividing the peak spectral acceleration prescribed by the code for non-structural elements possessing a period of vibration equal to that of the supporting structure by the peak acceleration of the supporting structure. Fig. 14(b) compares the 50<sup>th</sup> percentile values for the observed dynamic amplification factors with those predicted by Eqs.(4) and (5) and distinguishes between the amplification observed when the period of the supporting system lies near or far from the pulse period of the records.

Upon careful examination of the results presented in Fig. 14 it appears that records possessing velocity pulse characteristics do tend to increase the dynamic amplification factors. In particular,

note from Fig. 14(b) that for supporting systems with periods close to the pulse periods of the records (i.e., for  $1 \text{ s} < T_n < 2 \text{ s}$ ), the dynamic amplification factors are greater than those for other periods, particularly for low levels of elastic damping. At high levels of elastic damping the amplification factors appear to be unaffected by the pulse characteristics of the accelerograms. These observations suggest that the dynamic amplification predicted by Eq. (5) may need to be increased to account for records with pulse characteristics and this should be explored as part of future research. Nevertheless, one notes that the modification required to Eq. (5) would not need to be great and the new approach proposed here appears to perform considerably better than current code methods.

## 5. Conclusions

This paper has reviewed the need for current codes to incorporate improved methods of predicting floor response spectra for the design of secondary and non-structural elements. The focus of this paper has been on floor spectra atop SDOF supporting structures although it is also demonstrated in the first part of the paper that improvements are needed for both SDOF and MDOF systems. The concept of an apparent dynamic amplification factor is introduced to gauge the peak acceleration demands that secondary and non-structural elements could be subject to on SDOF supporting systems. An empirical expression for the dynamic amplification factor is proposed and successfully validated using the results of NLTH analyses of SDOF systems subject to 47 earthquake ground motions. A new series of empirical equations have then been proposed to predict floor spectra on SDOF supporting structures. The new empirical approach accounts for the period and inelasticity of the supporting structure to define the shape of the floor spectra and uses the elastic damping of the supported element in order to define the magnitude of the floor spectra. The results of NLTH analyses of a series of SDOF supporting structures subject to earthquake motions of varying intensity have indicated that the new methodology is very promising. The last part of the paper investigates the influence of ground motion characteristics on peak floor acceleration demands, examining apparent dynamic amplifications obtained for both long-duration records and records with velocity-pulses. The results suggest that dynamic amplification factors for long duration accelerograms may be similar to those obtained for normal duration records and that dynamic amplification factors may need to be magnified to account for the possibility of velocity pulses from near-source earthquake events. Summarizing, a new empirical expression for the dynamic amplification factor has been tested for a total of 75 accelerograms and the results show that the new expression could be very useful for design and is considerably better than current code approaches. The research has focused on floor response spectra atop SDOF systems with hysteretic properties typical of well detailed RC structures. Future research should explore the applicability of the approach for supporting systems with different hysteretic properties. Future research must also aim to extend the methodology to MDOF supporting structures in order to account for the effects of higher modes of vibration on floor response spectra.

## Acknowledgments

The authors wish to thank Elisa Zuccolo, Carlo Lai and Hossein Agha Beigi for providing long duration ground motions used in Section 4.1 of this study and Iunio Iervolino for providing the

near-source ground motions used in Section 4.2 of this study. The authors also wish to thank the anonymous reviewers for their careful comments and suggestions that significantly helped improve the quality of this paper.

## References

- ASCE/SEI 7-05 (2005), *Minimum design loads for buildings and other structures*, American Society of Civil Engineers, 388.
- Baker, J.W. (2007), “Quantitative classification of near-fault ground motions using wavelet analysis”, *B. Seismol. Soc. Am.*, **97**(5), 1486–1501.
- Carr, A.J. (2009), “Ruaumoko3D – A program for inelastic time-history analysis”, Department of Civil Engineering, University of Canterbury, New Zealand.
- CEN EC8 (2004), *Eurocode 8 – Design provisions for earthquake resistant structures*, EN-1998-1:2004: E, Comite Europeen de Normalization, Brussels, Belgium.
- Drake, R.M. and Bachman, R.E. (1995), “Interpretation of instrumented building seismic data and implications for building codes”, SEAOC.
- Chopra, A.K. (2000), *Dynamics of structures*, Pearson Education, USA.
- Dhakal, R.P. (2010), “Damage to non-structural components and contents in the 2010 Darfield earthquake”, *B. Earthq. Eng.*, **43**(4), 404-411.
- Emori, K. and Schnobrich, W.C. (1978), “Analysis of reinforced concrete frame-wall structures for strong motion earthquakes”, Civil Engineering Studies, Structural Research Series No.434, University of Illinois, Urbana, Illinois.
- Filiatrault, A., Epperson, M. and Folz, B. (2004), “Equivalent elastic modelling for the direct displacement-based seismic design of wood structures”, *ISET J. Earthq. Technol.*, **41**(1), 75-99.
- Igusa, T. and Der Kiureghian, A. (1985), “Generation of floor response spectra including oscillator-structure interaction”, *Earthq. Eng. Struct. D.*, **13**(5), 661-676.
- Kramer, S.L. (1996), *Geotechnical earthquake engineering*, Prentice-Hall.
- Krawinkler, H., Cofie, N.G., Astiz, M.A. and Kircher, C.A. (1979), “Experimental study on the seismic behaviour of industrial storage racks”, Report 41, John A. Blume Earthquake Engineering Center, Stanford University, California, 147.
- Kumari, R. and Gupta, V.K. (2007), “A modal combination rule for peak floor accelerations in multistoried buildings”, *ISET J. Earthq. Technol.*, **44**(1), 213–231.
- Lago, A. and Sullivan, T.J. (2011), “A review of glass façade systems and research into the seismic design of frameless glass façades”, IUSS Research Report No. ROSE-2011/01, IUSS press, Pavia, Italy, [www.iusspress.it](http://www.iusspress.it), 166.
- Lenk, P. and Coult, G. (2010), “Damping of glass structures and components”, *Proceedings of Challenging Glass Conference 2*, Delft, The Netherlands.
- Magenes, G., Morandi, P. and Penna, A. (2008), “Experimental in-plane cyclic response of masonry walls with clay units”, *Proceedings of the 14<sup>th</sup> World Conference on Earthquake Engineering*, Beijing, China.
- Menon, A. and Magenes, G. (2008), “Out-of-plane seismic response of unreinforced masonry definition of seismic input”, Research Report ROSE – 2008/04, IUSS Press, Pavia, Italy, 269.
- Nakagami, Y. (2003), “Probabilistic dynamics of wind excitation on glass façade”, Doctoral Thesis, University of Darmstadt, Germany.
- Newton, I. (1687), “*Philosophiae naturalis principia mathematica* (“Mathematical Principles of Natural Philosophy”)”, London; for an English version from 1846 see: <http://www.archive.org/details/newtonspmathema00newtrich>.
- NZS1170.5:2004 (2004), *Structural design actions Part 5 : Earthquake actions – New Zealand*, Standards Council of New Zealand.

- Otani, S. (1981), "Hysteretic models for reinforced concrete for earthquake analysis", *J. Fac. Architect.*, **36**(2), 125-159.
- Paulay, T. and Priestley, M.J.N. (1992), *Seismic design of reinforced concrete and masonry buildings*, John Wiley & Sons, Inc., New York.
- Priestley, M.J.N., Calvi, G.M. and Kowalsky, M.J. (2007), "Direct displacement-based seismic design", IUSS Press, Pavia, Italy, 720.
- Rivera, J. (2008), "On the development of seismic design forces for flexible floor diaphragms in reinforced concrete wall buildings", *ROSE School PhD thesis*, Univeristà degli Studi di Pavia, Pavia, Italy, 225.
- Rodriguez, M., Restrepo, J.I. and Carr, A.J. (2000), "Earthquake resistant precast concrete buildings: Floor accelerations in buildings", Department of Civil Engineering, University of Canterbury, Research Report 2000-6.
- Rodriguez, M.E., Restrepo, J.I. and Carr, A.J. (2002), "Earthquake-induced floor horizontal accelerations in buildings", *Earthq. Eng. Struct. D.*, **31**(3), 693-718.
- Seismosoft (2011), "SeismoSignal - A computer program for signal processing of strong-motion data", available from URL: <http://www.seismosoft.com>.
- Shelton, R.H., Park, S.G. and King, A.B. (2002), "Earthquake response of building parts", *Proceedings of NZ Society for Earthquake Engineering Annual Conference*.
- Sullivan, T.J., Priestley, M.J.N. and Calvi, G.M. (2006), "Seismic design of frame-wall structures", ROSE Research Report 2006/02, IUSS Press, Pavia, Italy.
- Taghavi, S. and Miranda, E. (2006), "Seismic demand assessment on acceleration-sensitive building non-structural components", *Proceedings of the 8th National Conference on Earthquake Engineering*, San Francisco, California, USA.
- The New Zealand Treasury (2011) "Budget economic and fiscal update 2011", ISBN: 978-0-478-37812-2 (Online) <http://purl.oclc.org/nzt/b-1381>.
- Thomson, W.T. and Dahleh, M.D. (1998), "Theory of vibration with applications", Fifth Edition, Prentice Hall, Upper Saddle River, New Jersey 07458, U.S., 524.
- Villaverde, R. (1997), "Seismic design of secondary structures: state of the art", *J. Struct. Eng.-ASCE*, **123**(8), 1011-1019.
- Villaverde, R. (2004), "Seismic analysis and design of non-structural elements", in *Earthquake engineering from engineering seismology to performance-based design*, (Eds) Y. Bozorgnia, V.V. Bertero, CRC Press, 19-48.